Biochemical Pharmacology 79 (2010) 596–609

Contents lists available at ScienceDirect

Biochemical Pharmacology

journal homepage: www.elsevier.com/locate/biochempharm

A novel anti-neuroinflammatory pyridylimidazole compound KR-31360

Jiyeon Ock [a], Sangseop Kim [a,1], Kyu-Yang Yi [b], Nak-Jung Kim [b], Hyung Soo Han [c], Je-Yoel Cho [d], Kyoungho Suk [a,*]

[a] Department of Pharmacology, School of Medicine, Brain Science and Engineering Institute, CMRI, Kyungpook National University, 101 Dong-In, Joong-gu, Daegu 700-422, Republic of Korea
[b] Medical Science Division, Korea Research Institute of Chemical Technology, Daejeon, Republic of Korea
[c] Department of Physiology, School of Medicine, Kyungpook National University, Daegu, Republic of Korea
[d] Department of Biochemistry, School of Dentistry, Kyungpook National University, Daegu, Republic of Korea

ARTICLE INFO

Article history:
Received 10 August 2009
Received in revised form 23 September 2009
Accepted 23 September 2009

Keywords:
Neuroinflammation
Microglia
Neuroprotection
Neurodegenerative disease
Pyridylimidazole compound
TLR pathway

ABSTRACT

Excessive microglial activation with overexpression of proinflammatory cytokines and oxidative stress products is linked to the progression of several neurodegenerative diseases; therefore, suppression of microglial activation is a potential therapeutic approach against these diseases. Since nitric oxide (NO) is one of the major inflammatory mediators that are produced by activated microglia, inhibitory effects of novel synthetic compounds on microglial NO production were investigated. From the mouse microglia cell-based assays, an imidazo [4,5-b] pyridine compound KR-31360 was identified as an inhibitor of microglial NO production with an IC_{50} value of 2 μM. Structure–activity relationship study indicated that 5-position of imidazo [4,5-b] pyridine ring is critical for the activity. KR-31360 also inhibited lipopolysaccharide (LPS)-induced secretion of tumor necrosis factor alpha (TNF-α) and transcription of TNF-α, interleukin-1 beta, and inducible nitric oxide synthase as well as activation of nuclear factor kappa B and mitogen-activated protein kinases. KR-31360 was neuroprotective by suppressing microglial neurotoxicity in a microglia–neuron coculture. The neuroprotective activity of the compound was most effective when microglia were pretreated with the compound prior to LPS challenge. The inhibitory effect of KR-31360 on microglial activation was further demonstrated in a mouse neuroinflammation model *in vivo*: compared to vehicle-injected animals, KR-31360 injection attenuated LPS-induced microglial activation as evidenced by isolectin B4 staining and proinflammatory gene expression of brain sections. DNA microarray analysis supported that KR-31360 targeted Toll-like receptor 4 pathways. In addition to being a new drug candidate against neuroinflammatory diseases, the compound may be a powerful tool for the better understanding of microglia biology and neuroinflammation.

1. Introduction

Inflammation in the brain was once regarded as only a passive response to neuronal damage. However, increasing evidence now indicates that inflammation is capable of actively causing neuronal death and damage, which in turn fuels a self-perpetuating cycle of neurodegeneration [1]. Thus, while the triggers of various neurodegenerative diseases are diverse, inflammation may be a crucial mechanism driving the progressive nature of several neurodegenerative diseases such as Alzheimer's disease, Parkinson's disease, and multiple sclerosis. Although it is thought that several cell types contribute to inflammation-mediated neurodegeneration, microglia have been implicated as critical components of the immunological insult to neurons [2]. Microglia are the resident immune cells of the central nervous systems (CNS), and serve the role of immune surveillance and host defense under physiological conditions [3]. However, microglia become activated in response to brain infection or injury, and up-regulate a variety of surface receptors including the major histocompatibility complex and complement receptors. They also secrete neurotrophic factors, which are potentially beneficial to the survival of neurons [4]. The majority of factors produced by over-activated microglia, however, are proinflammatory and neurotoxic in nature. These include the cytokines tumor necrosis factor alpha (TNF-α) and interleukin 1 beta (IL-1β) and free radicals such as nitric oxide (NO) and superoxide anion, which may contribute to neuronal injuries

* Corresponding author. Tel.: +82 53 420 4835; fax: +82 53 256 1566.
E-mail address: ksuk@knu.ac.kr (K. Suk).
[1] Present address: Division of Laboratory Animal Resources, National Institute of Toxicological Research, Korea FDA, Seoul, Republic of Korea.

0006-2952/$ – see front matter © 2009 Elsevier Inc. All rights reserved.
doi:10.1016/j.bcp.2009.09.026

and progression of neurodegenerative diseases [5]. Although the relationship between microglial activation and neurodegenerative diseases is not completely understood, it is now generally accepted that microglial activation is actively involved in the initiation and progression of multiple neurodegenerative diseases [6,7]. Thus, the inhibition of microglial activation would be an effective therapeutic approach to alleviating the progression of neurodegenerative diseases.

The Toll-like receptors (TLR) family is an important recognition and signaling component of mammalian host defense, and it initiates innate immune responses upon interaction with various pathogens [1]. It is known that microglia express TLRs 1–9 [8] and some of these receptors are related to microglial activation and neurotoxicity [1]. TLR signaling is initiated by the conserved Toll-IL-1 receptor (TIR) domain, which mediates recruitment of TIR domain-containing adaptor proteins. These proteins activate two main signal transduction pathways; MyD88-dependent and MyD88-independent pathways, which lead to the transcriptional expression of proinflammatory cytokines and interferons [9]. Thus, modulation of TLR signaling might be a potential strategy to regulate microglial activation and ultimately neurotoxicity.

Here, a small molecule library containing 6480 different skeletal structures was screened for the anti-neuroinflammatory activity using microglia cell-based assay. From this initial screening, imidazo [4,5-b] pyridine compounds showed the greatest activity with an IC_{50} value of around 10 μM (data not shown). In order to find more potent inhibitors, several derivatives of imidazo [4,5-b] pyridine series were rescreened using the same assay. From the secondary microglia cell-based screening, KR-31360 was identified as a potent inhibitor of microglial activation with an IC_{50} value of 2 μM. KR-31360 markedly reduced the expression of several proinflammatory mediators at mRNA and protein levels. In addition, this compound inhibited the activation of nuclear factor kappa B (NF-κB), extracellular signal-regulated kinase (ERK), and c-jun N-terminal kinase (JNK) in the downstream of TLR4, which was further supported by DNA microarray analyses. KR-31360 also showed a protective effect against microglia-mediated neurotoxicity in the coculture model, and exerted microglia inhibitory effects in a neuroinflammation model *in vivo*.

2. Materials and methods

2.1. Reagents and cell culture

Bacterial lipopolysaccharide (LPS) from *Escherichia coli* 0111:B4 and adenosine 5′-triphosphate (ATP) disodium salt were obtained from Sigma (St. Louis, MO, USA). Recombinant mouse interferon-gamma (IFN-γ) was purchased from R&D Systems (Minneapolis, MN, USA). Synthetic chemical compounds of imidazo [4,5-b] pyridine series were originally synthesized by Dr. Sung-Eun Yoo at Korea Research Institute of Chemical Technology (Daejeon, Korea) [10] and obtained through the Korea Chemical Bank (Daejeon, Korea). These compounds were solubilized in dimethyl sulfoxide (DMSO) and added to the cell culture at the desired concentrations. The immortalized BV-2 murine microglial cell line [11] which exhibits phenotypic and functional properties comparable to those of primary microglial cells [12] was maintained in Dulbecco's modified Eagle's medium (DMEM; BioWhittaker, Walkersville, MD, USA) containing 5% heat-inactivated FBS and 50 μg/ml gentamicin at 37 °C. The highly aggressively proliferating immortalized (HAPI) rat microglial cell line [13], RAW 264.7 mouse macrophage cell line (ATCC, TBI-71), and B35 rat neuroblastoma cell line (ATCC, CRL-2754) [14] stably expressing enhanced green fluorescent protein (EGFP) [15] were maintained in DMEM containing 10% heat-inactivated FBS, 2 mM glutamine, 10 U/ml penicillin, and 10 μg/ml streptomycin (Gibco-BRL, Gaithersburg, MD, USA) at 37 °C under a humidified atmosphere with 5% CO_2. Mouse primary microglial cultures were prepared by mild trypsinization as previously described with minor modifications [16]. In brief, the forebrains of newborn Institute of Cancer Research (ICR) mice were chopped and dissociated by mechanical disruption using a nylon mesh. The cells were seeded into poly-L-lysine-coated flasks. After *in vitro* culture for 10–14 days, microglial cells were isolated from mixed glial cultures by mild trypsinization. Mixed glial cultures were incubated with a trypsin solution [0.25% trypsin, 1 mM EDTA in Hank's balanced salt solution (HBSS)] diluted 1:4 in phosphate-buffered saline (PBS; 150 mM NaCl, 5 mM phosphate, pH 7.4) containing 1 mM $CaCl_2$ for 30–60 min. This resulted in the detachment of an upper layer of astrocytes in one piece, whereas the microglia remained attached to the bottom of the culture flask. The detached layer of astrocytes was aspirated, and the remaining microglia were used for experiments. The purity of microglial cultures was greater than 95% as determined by isolectin B4 staining (data not shown). Primary cultures of dissociated cerebral cortical neurons were prepared from embryonic day 20 (E20) ICR mice as described previously [17]. Briefly, mouse embryos were decapitated, and the brains were rapidly removed and placed in a culture dish with cold PBS. The cortices were isolated and then transferred to a culture dish containing 0.25% trypsin–EDTA (Gibco-BRL) in PBS for 30 min at 37 °C. After two washes in serum-free neurobasal media (Gibco-BRL), the cortical tissues were mechanically dissociated with a gentle pipetting. Dissociated cortical cells were seeded onto poly D-lysine coated plates using neurobasal media containing 10% FBS, 0.5 mM glutamine, 100 U/ml penicillin, 100 μg/ml streptomycin, N2 supplement (Gibco-BRL), and B27 supplement (Gibco-BRL). Cells were maintained by changing the media every 2–3 days and grown at 37 °C in a 5% CO_2 humidified atmosphere. The purity of neuronal cultures was determined by immunocytochemical staining using an antibody against a neuron-specific marker, microtubule-associated protein 2 (MAP2; Promega, Madison, WI, USA). The animals were maintained under temperature- and humidity-controlled conditions with a 12-h light/12-h dark cycle. All animal experiments were approved by the Institutional Review Board of Kyungpook National University School of Medicine and were carried out in accordance with the guidelines in the NIH Guide for the Care and Use of Laboratory Animals.

2.2. Nitrite quantification

The production of NO was estimated by measuring the amount of nitrite, a stable metabolite of NO. Cells were treated with LPS, IFN-γ, or ATP in the absence or presence of chemical compound(s). At the end of the 24 h incubation, 50 μl of the cell culture media were mixed with an equal volume of a Griess reagent (0.1% naphthylethylenediamine dihydrochloride and 1% sulfanilamide in 5% phosphoric acid) in a 96-well microtiter plate. Light absorbance was read at 540 nm and the sodium nitrite was used to prepare a standard curve.

2.3. Cell viability assessment

Cell viability was assessed by a modified 3-(4,5-dimethylthiazol-2-yl)-2,5-diphenyltetrazolium bromide (MTT) assay, as previously described [18].

2.4. TNF-α ELISA

BV-2 cells were treated with LPS in the absence or presence of KR-31360. After 24 h incubation, the levels of TNF-α in culture media were measured with rat monoclonal anti-mouse TNF-α antibody as capture antibody and goat biotinylated polyclonal

Table 1
Primer sequences used for RT-PCR.

Gene	Forward primer	Reverse primer	Product size (bp)
β-actin	5′-ATC CTG AAA GAC CTC TAT GC-3′	5′-AAC GCA GCT CAG TAA CAG TC-3′	287
CDK4	5′-TGG CTG CC CTC GAT ATG AAC-3′	5′-CCT CAG GTC CTG GTC TAT ATG-3′	302
CK1ε	5′-GCC TCT GGT GAG GAA GTA G-3′	5′-CGG TAG GGA ATA TGC TGG TG-3′	416
IKKε	5′-GTA CAG AAT CAC CAC AGA GAA GC-3′	5′-GAC CTG CTG AAC AGA GTT AGA GG-3′	453
IL-1β	5′-GCA ACT GTT CCT GAA CTC-3′	5′-CTC GGA GCC TGT AGT GCA-3′	382
iNOS	5′-CCC TTC CGA AGT TTC TGG CAG CAG C-3′	5′-GGC TGT CAG AGC CTC GTG GCT-3′	497
MCP-1	5′-CAG CAG GTG TCC CAA AGA-3′	5′-CTT GAG GTG GTT GTG GAA A-3′	253
MIP-1α	5′-TCT GCA ACC AAG TCT TCT CAG-3′	5′-GAA GAG TCC CTC GAT GTG GGC TA-3′	373
PPARα	5′-ACC TTG CTA AAG TAC GGT GTG TA-3′	5′-GCA ACT TGT CAA TGT AGC CTA TG-3′	283
TNF-α	5′-CAT CTT CTC AAA ATT CGA GTG ACA A-3′	5′-ACT TGG GCA GAT TGA CCT CAG-3′	411

anti-mouse TNF-α antibody as a detection antibody (ELISA development reagent; R&D Systems) as previously described [15].

2.5. Reverse transcription-polymerase chain reaction (RT-PCR)

Total RNA was extracted using TRIZOL (Invitrogen, Carlsbad, CA, USA). Reverse transcription was carried out using 0.5 μg of total RNA, 0.75 pmol of oligo(dT) primer, 1 unit of RNase inhibitor (Promega), 0.5 mM dNTPs, and 20 units of M-MLV reverse transcriptase (Promega) in reaction buffer containing 50 mM Tris–HCl (pH 8.3), 75 mM KCl, 3 mM $MgCl_2$, and 10 mM DTT at 37 °C for 1 h. PCR amplification was carried out in 50 μl PCR reaction mixture containing 10 mM Tris–HCl (pH 8.3), 50 mM KCl, 2 mM $MgCl_2$, 20 pmol primer sets, 2 units of Taq DNA polymerase (CoreBio System Co., Seoul, Korea), 0.2 mM dNTPs, and 2 μl of cDNA reaction. PCR amplification using primer sets specific for inducible nitric oxide synthase (iNOS), TNF-α, IL-1β, casein kinase 1 epsilon (CK1ε), inhibitor of kappa B kinase epsilon (IKKε), or β-actin was carried out at 94 °C for 30 s, 55 °C for 30 s, and 72 °C for 1 min, and repeated for 23 cycles followed by incubation at 72 °C for 7 min. PCR for peroxisome proliferator-activated receptor alpha (PPARα) and cyclin-dependent kinase 4 (CDK4) was carried out at 94 °C for 30 s, 60 °C for 30 s, and 72 °C for 1 min, and repeated for 25 cycles followed by incubation at 72 °C for 7 min. PCR cycle for monocyte chemoattractant protein 1 (MCP-1) or macrophage inflammatory protein 1 alpha (MIP-1α) was 28 or 32, respectively, under the same condition. Nucleotide sequences of the primers were described in Table 1. For the analysis of PCR products, 10 μl of each PCR reaction was electrophoresed on 1% agarose gel and visualized by ethidium bromide staining. The β-actin was used as an internal control to evaluate relative expression of the examined genes.

2.6. Western blot analysis

BV-2 cells were pretreated with KR-31360 for 30 min and stimulated with LPS. After LPS stimulation for 15, 30, and 60 min, cells were washed with PBS and lysed with lysis buffer [50 mM Tris–HCl (pH 8.0), 150 mM NaCl, 0.02% sodium azide, 0.1% sodium dodecyl sulfate (SDS), 1% Nonidet P-40, 1 mM phenylmethylsulfonyl fluoride]. Equal amounts of protein were separated by SDS-polyacrylamide gel electrophoresis (12% gel) and transferred to nitrocellulose membranes (Amersham Biosciences, Piscataway, NJ, USA). The membranes were blocked with 5% skim milk in Tris-buffered saline Tween-20 (TBST) and then incubated with primary antibodies [polyclonal rabbit anti-phospho- or total forms of p38 mitogen-activated protein kinase (MAPK), c-jun N-terminal kinase (JNK), and p44/p42 ERK antibodies (Cell Signaling Technology Inc., Beverly, MA, USA), and monoclonal anti-α-tubulin clone B-5-1-2 mouse ascites fluid (Sigma)]. After thoroughly washing with TBST, horseradish peroxidase-conjugated secondary antibodies were applied. The blots were developed by the enhanced chemiluminescence detection kit (ECL; Amersham Biosciences).

2.7. Immunofluorescence staining

BV-2 cells were cultured in sterile coverslips and pretreated with KR-31360 for 30 min and stimulated with LPS. After 1 h, coverslips were fixed in 4% paraformaldehyde for 30 min at room temperature and then in cold methanol for 10 min at −20 °C. Fixed cells were permeabilized in 0.3% Triton X-100/PBS for 10 min at room temperature, and then blocked in 1% normal horse serum. Afterwards, the cells were sequentially incubated with mouse anti-p65 antibody (1:100 dilution; Santa Cruz Biotechnology Inc., Santa Cruz, CA, USA) at 4 °C overnight and Alexa Fluor-488 labeled goat anti-mouse IgG (1:2000 dilution; Molecular Probes Inc., Eugene, OR, USA) at room temperature for 1 h. Cells were washed with PBS containing 0.05% Tween-20, and then stained with 0.5 μg/ml Hoechst 33342 solution (Molecular Probes) for 20 min at 37 °C. Stained cells were mounted in a 1:1 mixture of xylene and malinol and examined on a fluorescent microscope. For the staining of actin cytoskeleton, fixed microglia cells were incubated in PBS containing 3% BSA and 0.12 g/ml of TRITC (tetramethylrhodamine isothiocyanate)-conjugated phalloidin (Actin cytoskeleton and focal adhesion staining kit; Millipore Bioscience Research Reagents, Temecula, CA, USA) at room temperature for 30 min. After three washes in PBS containing 0.05% Tween-20, cells were incubated with 0.5 μg/ml of Hoechst 33342 fluorochrome (Molecular Probes). The samples were mounted and observed by means of confocal microscopy (Zeiss LSM 510; Oberkochen, Germany).

2.8. Electrophoretic mobility shift assay (EMSA)

BV-2 cells were pretreated with KR-31360 for 30 min and stimulated with LPS for 1 h. The nuclear extracts were then subjected to EMSA as previously described [19].

2.9. Microglia–neuron coculture

Microglia–neuron coculture was done using either HAPI rat microglia cells and B35 rat neuroblastoma cells or primary microglia and neurons. HAPI rat microglia cells were plated at a density of 1.5×10^4 cells/well in 96-well plate and allowed to adhere for 4 h and then the cells were treated with KR-31360 for 30 min. After incubation, media were removed and cells were washed with PBS. EGFP-transfected B35 rat neuroblastoma cells (3.75×10^4 cells/well) were added to HAPI cell-plated wells in conjunction with culture media containing LPS. The numerical ratio of microglia to neuroblastoma was 1:2.5. After an additional 24 h incubation period, the number of EGFP-positive cells was counted at a 100-fold magnification in four visual fields in each well using a fluorescence microscope (Olympus IX 70 inverted fluorescence microscope, Tokyo, Japan) equipped with a cooled CCD camera. Images of five random fields per well were captured and analyzed by the MetaMorph imaging system (Universal Imaging Corp., West Chester, PA, USA). For the MTT viability assay, HAPI cells were treated with KR-31360 at different time points: pretreatment for 30 min before

the challenge of LPS; cotreatment with LPS; or posttreatment for 30 min after the challenge of LPS. After LPS treatment for 24 h, microglia–neuroblastoma coculture was subjected to MTT assay as described above. For the coculture of primary microglia and primary cortical neurons, primary mouse microglia cultures were treated with KR-31360 for 30 min. After incubation, media were removed and cells were washed with PBS. CellTracker Green 5-chloromethylfluorescein diacetate (CMFDA; Molecular Probes)-labeled mouse primary cortical neurons were added to microglia-plated wells in conjunction with culture media containing LPS. For the chronic stimulation of microglial cultures, culture media were replaced with fresh media containing LPS every 24 h over a 72 h period. After incubation, the number of CMFDA-positive cells was counted using a fluorescence microscope.

2.10. Microglia-conditioned media

Primary microglia cultures were treated for 6 h with LPS in the absence or presence of KR-31360. After incubation, culture media were replaced by fresh culture media and incubated for 24 h. Conditioned media were collected and centrifuged at 13,000 rpm for 5 min to remove cellular debris. Primary cortical neurons were plated at a density of 4×10^4 cells per well in 100 μl of media in 96-well plates and allowed to settle at 37 °C for 24 h before addition of primary microglia-conditioned media. Primary cortical neurons were incubated at 37 °C for a further 24 h. Cell viability was measured by MTT assay as described above.

2.11. Mouse model of neuroinflammation

Peripheral injection of LPS was done to evoke neuroinflammation in mice as previously described [20,21]. All experiments were carried out on 11-week-old male C57BL/6 mice (25–30 g), supplied by Koatech (Pyongtaec, Korea). Mice were divided into three experimental groups in each experiment: (1) normal group of mice were not administered with any reagent; (2) KR-31360 + LPS group of mice were administered with LPS and KR-31360 diluted in PBS; and (3) vehicle + LPS group of mice were administered with LPS and 0.5% DMSO diluted in PBS. DMSO was included in the vehicle, because KR-31360 was dissolved in DMSO. KR-31360 (20 mg/kg) or vehicle (PBS containing 0.5% DMSO) was administered intraperitoneally once daily for 4 days. LPS (from *E. coli* 055:B5; Sigma–Aldrich) was administered intraperitoneally at a dose of 5 mg/kg on day 2 for a single challenge. For histochemical analysis, mice were anesthetized at 72 h after the LPS injection (day 5), and then transcardially perfused with saline and fixed in 4% paraformaldehyde for 72 h. For mRNA analysis, mice were anesthetized at 6 h after LPS injection, and transcardially perfused with saline. The brains were removed and stored at −80 °C until analysis. At least three animals were used for each experimental group.

2.12. Histochemistry

Paraformaldehyde-fixed brain tissues were coronal-sectioned into three parts and embedded in paraffin, which were then cut at 6 μm thickness. After deparaffinization and antigen retrieval by boiling in 10 mM citric acid solution (pH 6.0), sections were treated with 0.03% H_2O_2 to remove endogenous peroxidase activity. The sections were then incubated with peroxidase-labeled isolectin B4 from *Bandeiraea simplicifolia* (IB4, 1:100, Sigma–Aldrich) and detected using the liquid DAB+ chromogenic-substrate system (Dakocytomation, Copenhagen, Denmark). Stained sections were dehydrated and mounted. In the IB4-stained sections, positive cells were counted in a blinded fashion from randomly selected ten fields for each brain section of animal at 200× magnification. Brain regions selected for counts were five adjacent fields of cortex, three adjacent fields of hippocampus, and two adjacent fields of substantia nigra. These ten fields were visualized at the same position in each brain section. Then, the number of IB4-positive cells per square millimeter was calculated according to the size of the specific brain area. For staining with NeuN, sections were incubated with peroxidase-labeled primary antibody against NeuN (1:600; Chemicon, Temecula, CA, USA) and detected using the liquid DAB+ chromogenic-substrate system (Dakocytomation).

2.13. DNA microarray analysis: preparation of fluorescent DNA probe and hybridization

BV-2 cells were plated at a density of 1×10^6 cells/well in 6-well plates, allowed to adhere for 4 h, and then treated with LPS in the absence or presence of KR-31360 for 4 h. Total RNA was extracted using TRIZOL (Invitrogen). Total RNA sample (40 μg) was labeled with either Cyanine 3 (Cy3)- or Cyanine 5 (Cy5)-conjugated dCTP (Amersham) by a reverse transcription reaction using reverse transcriptase SuperScript II (Invitrogen). The labeled cDNA mixture was then concentrated using an ethanol precipitation method. The concentrated Cy3 and Cy5 labeled cDNAs were resuspended in 10 μl of hybridization solution (GenoCheck, Ansan, Korea). After the two labeled cDNAs were mixed, they were placed on OpArray Mouse genome 35k chip (OPMMV4, Operon Biotechnologies, GmbH) and covered by a MAUI FL chamber (Biomicro Systems, Inc., Salt Lake City, UT, USA). The slides were hybridized for 16 h at 42 °C by using MAUI hybridization system (Biomicro Systems, Inc.). The hybridized slides were washed with 2× SSC, 0.1% SDS for 2 min, 1× SSC for 3 min, and then 0.2× SSC for 2 min at room temperature. The slides were dried by centrifugation at 890 × *g* for 20 s.

2.14. Microarray data analysis

Hybridized slides were scanned with the GenePix 4000B scanner (Axon Instruments, Union City, CA, USA). The scanned images were analyzed with the software program GenePix Pro 5.1 (Axon Instruments) and GeneSpring 7.2 (Sillicongenetics, Redwood City, CA, USA). Spots that were judged as substandard by visual examination of each slide were flagged and excluded from further analysis. Spots that had dust artifacts or spatial defects were manually flagged and excluded. To filter out the unreliable data, spots with signal-to-noise [signal − background; background standard deviation (SD)] below 10 were not included in the data. Data were normalized by global lowess, print-tip lowess, and scaled normalization for data reliability. Fold change filters included the requirement that the genes be present in at least 150% of controls for up-regulated genes and lower than 50% of controls for down-regulated genes. The accuracy of microarray analyses in this study was confirmed by RT-PCR. GenPlex™ v3.0 software (Istech Inc., Goyang, Korea) was used for pathway analysis of microarray data, where probe ID of each gene in platform of Operon chip was utilized. Gene mapping on the pathway (Fig. 7) was performed using the Kyoto Encyclopedia of Genes and Genomes (KEGG) pathway database.

2.15. Two-dimensional gel electrophoresis (2-DE) and protein identification

BV-2 cells were cultured in the absence or presence of KR-31360 for 24 h. After treatment, cells were washed with low-salt washing solution (10 mM Tris–HCl, 250 mM sucrose, pH 7.0) and lysed with lysis buffer (7 M urea, 2 M thiourea, 4% CHAPS, and 40 mM DTT). Proteins (80 μg) were solubilized in rehydration sample buffer (7 M urea, 2 M thiourea, 2% CHAPS, 100 mM DTT, 1% IPG buffer, and 0.002% bromophenol blue) and applied onto 18 cm IPG strips (Amersham Biosciences, pH 3–10, NL). Isoelectrofocus-

ing (IEF) was performed for 1 h at 200 V, 1 h at 500 V, 1 h at 1000 V, 1 h at 8000 V, and 80,000 Vh. Thereafter, the IPG strips were equilibrated for 15 min in SDS equilibration buffer A [50 mM Tris–HCl (pH 8.8), 6 M urea, 30% glycerol, 2% SDS, 1% DTT, 0.002% bromophenol blue] and then for 15 min in SDS equilibration buffer B [50 mM Tris–HCl (pH 8.8), 6 M urea, 30% glycerol, 2% SDS, 2% iodoacetamide, 0.002% bromophenol blue]. For the second dimension separation, vertical slab gels (12% SDS PAGE) were employed. An equilibrated IPG gel strip was laid on top of the gel and sealed with 0.5% agarose solution. Gel electrophoresis was carried out at 16 °C at 30 mA/cm for 30 min and at 50 mA/cm until the bromophenol blue reached the bottom of the gel. The gel was fixed in 50% methanol and 12% acetic acid for overnight at 4 °C. Proteins were detected by silver-staining as previously described [22] and the protein spots were compared. Protein identification was done by liquid chromatography–mass spectrometry/mass spectrometry (LC–MS/MS) as previously described [23].

2.16. Statistical analysis

All data were presented as mean ± S.D. from three or more independent experiments, unless stated otherwise. Statistical comparisons between different treatments were done by either a Student's *t*-test or one-way ANOVA with Bonferroni's post hoc tests by using the SPSS version 14.0K program (SPSS Inc., Chicago, IL, USA). Differences with a value of $P < 0.05$ were considered to be statistically significant.

3. Results

3.1. Screening of imidazo [4,5-b] pyridine compounds as inhibitors of LPS-induced microglial activation and structure–activity relationship (SAR) study

Among many inflammatory mediators produced by activated microglia, NO production has been widely used as a representative measure of inflammatory activation of microglia [24,25]. Therefore, the suppressive effect of small molecule compounds of imidazo [4,5-b] pyridine series on LPS-induced NO production was investigated. When the BV-2 mouse microglia cells were treated with increasing concentration of LPS, 100 ng/ml was found to be the optimal concentration to induce NO production. The concentration of LPS higher than 100 ng/ml did not further increase the magnitude of the response (Fig. 1A). Therefore, 100 ng/ml of LPS was used throughout the experiments. BV-2 microglia cells were stimulated with LPS (100 ng/ml) in the presence or absence of chemical compounds for 24 h. The accumulated nitrite in the culture media, estimated by Griess reaction, was used as an index for NO synthesis. As shown in Fig. 1B, imidazo [4,5-b] pyridine derivatives KR-31360 and KR-35048 significantly inhibited the NO production in LPS-stimulated BV-2 cells at a concentration of 2 μM (summarized in Table 2; the skeletal structure of the compounds is shown in Fig. 1C). Upon screening of nine imidazo [4,5-b] pyridine derivatives, KR-31360 showed the greatest suppressive effect on LPS-induced NO production in BV-2 cells without apparent cytotoxicity (Fig. 1B). The microglia inhibitory effect of KR-31360 was further confirmed at several different concentrations using BV-2 microglia cells, HAPI microglia cells, RAW 264.7 macrophage cells, and mouse primary microglia cultures (Fig. 2A). KR-31360 also inhibited NO production in ATP-stimulated BV-2 microglial cells. However, the compound did not significantly inhibit IFN-γ-induced NO production (Fig. 2B), indicating the selective modulation of microglial signaling by KR-31360. These compounds are imidazopyridine derivatives that have biphenyltetrazole group at the 1-position of imidazopyridine ring. The 2-position of imidazo [4,5-b] pyridine ring was substituted by the

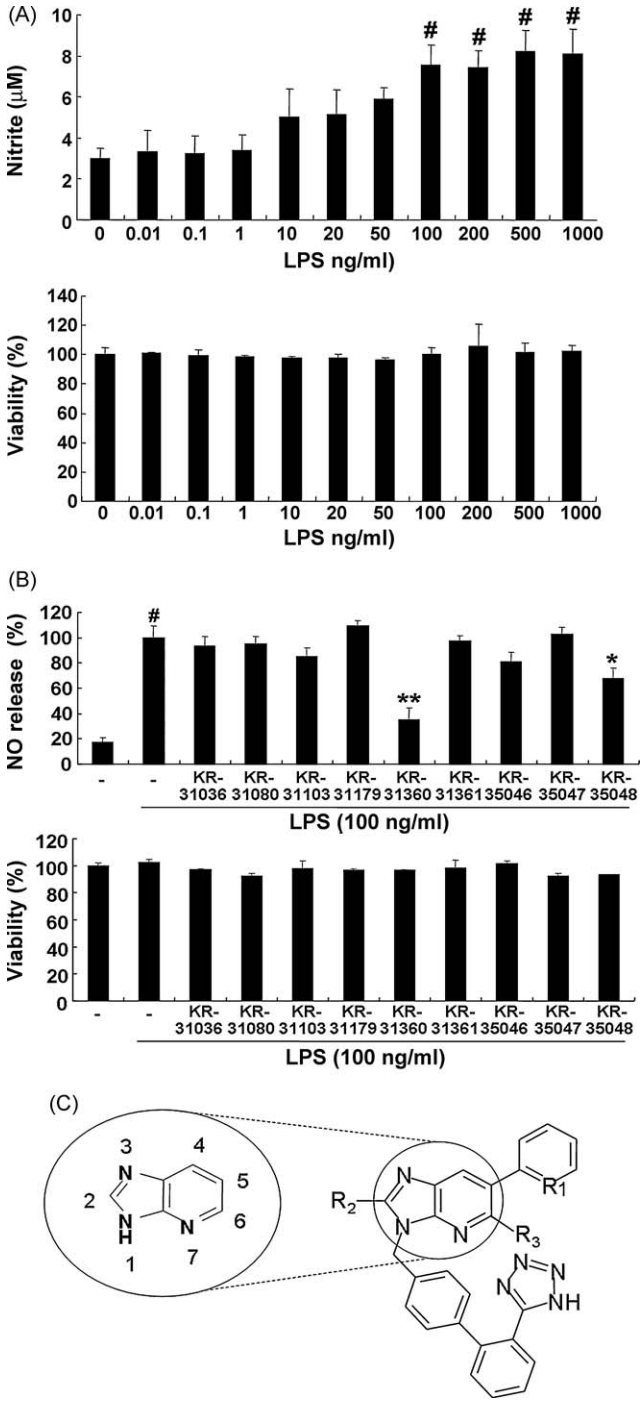

Fig. 1. The effect of imidazo [4,5-b] pyridine derivatives on NO production in LPS-stimulated BV-2 microglia cells. BV-2 microglia cells were treated with LPS in the absence or presence of the compounds (2 μM) for 24 h. Nitrite content in the culture media was measured using the Griess reaction and the results were expressed as either nitrite concentration or percentage of released NO from LPS-stimulated BV-2 cells (upper). Cytotoxicity was assessed by MTT assays and the results were expressed as percentage of surviving cells over control cells (lower). The LPS concentrations of higher than 100 ng/ml did not show a further increase in NO production (A). Among the compounds tested, KR-31360 most strongly reduced LPS-induced NO production (B; upper) without any cytotoxicity (B; lower) in BV-2 cells. The skeletal structure of imidazo [4,5-b] pyridine derivatives is shown (C). Structure of imidazopyridine ring and its numbering are also shown (C; enlarged). See Table 2 for a detailed chemical structure for the positions R1 to R3. The data were expressed as the mean ± S.D. ($n = 3$). $^{\#}P < 0.01$ vs. untreated control; $^{*}P < 0.05$, $^{**}P < 0.01$ vs. LPS only.

Table 2
Structure–activity relationship of imidazo [4,5-b] pyridine derivatives in the NO assay.

Compound ID[a]	R1	R2	R3	Inhibition (%)[b]
KR-31036	CH	C_4H_9	$CH(OC_4H_9)_2$	11.7 ± 6.0
KR-31080	NO^-	C_4H_9	CH_3	8.3 ± 4.3
KR-31103	NO^-	C_4H_9	CO_2CH_3	18.2 ± 5.4
KR-31179	NO^-	C_4H_9	$CH(OH)CH_3$	–
KR-31360	N	C_4H_9	CN	78.4 ± 6.9
KR-31361	NO^-	C_4H_9	CN	3.1 ± 3.2
KR-35046	N	C_4H_7	CH_3	24.8 ± 5.4
KR-35047	NO^-	C_4H_9	$CHCN(C_2H_5)$	–
KR-35048	NO^-	C_4H_9	CHO	44.8 ± 6.0

[a] All compounds were tested at 2 μM concentration. See Fig. 2 for the positions of R1 to R3 in the chemical structure.
[b] Results are mean ± SD ($n = 3$). Percent inhibition was based on following calculation: %inhibition = [(A − B)/(A − C)] × 100. A − C indicate NO_2^- concentrations (μM) under following conditions: A, LPS (+), compound (−); B, LPS (+), compound (+); C, LPS (−), compound (−).

butyl group in all compounds except KR-35046, which was substituted by the butenyl group. The 5-position of imidazo [4,5-b] pyridine ring was substituted by one group among phenyl, pyridine, and pyridine 1-oxide in each compound. The 6-position of imidazo [4,5-b] pyridine ring was substituted by various chemical groups. Through the structure–activity relationship studies, it was found that substituting the pyridine ring in the 5-position of imidazo [4,5-b] pyridine ring by pyridine 1-oxide resulted in a significant decrease in the inhibitory activities of synthetic compounds (Table 2).

3.2. Effect of KR-31360 on LPS-induced proinflammatory gene expression in microglial cells

In the CNS, TNF-α is a proinflammatory cytokine produced primarily from activated microglia and is involved in pathogenesis and/or the exacerbation of brain inflammation. To investigate the inhibitory effect of KR-31360 on the production of TNF-α, BV-2 microglia cells were incubated with LPS (100 ng/ml) in the absence or presence of KR-31360 (2 μM) for 24 h, and the levels of TNF-α were measured in the culture media by ELISA. Compared to unstimulated cells, the TNF-α levels were increased in the culture media of LPS-stimulated BV-2 cells, which were reduced 66.4 ± 2.8% by treatment with KR-31360 (Fig. 2C). The iNOS expression is induced in activated microglia and mediates synthesis of large amounts of NO. Levels of proinflammatory cytokines such as TNF-α and IL-1β are also increased in activated microglia. Therefore, the effect of KR-31360 on IL-1β, iNOS, and TNF-α gene expression at transcriptional levels was determined by RT-PCR. Based on the previous studies that examined microglial gene expression [26–28], the transcriptional level of the proinflammatory genes was determined at 6 h after LPS treatment. The mRNA levels of these proinflammatory genes in LPS-stimulated BV-2 cells were significantly reduced by KR-31360 (Fig. 2D). The compound alone did not significantly affect the expression level of these genes.

3.3. Effect of KR-31360 on LPS-induced NF-κB activation and MAPKs phosphorylation in microglial cells

Since NF-κB has been implicated in the transcriptional activation of various proinflammatory cytokines and iNOS [29], the effects of KR-31360 on this signaling pathway were examined by immunofluorescence staining of NF-κB p65 and electrophoretic mobility shift assay. In resting cells, NF-κB/IκB complexes are present in the cytoplasm. Activation of cells under the appropriate condition leads to phosphorylation and subsequent degradation of IκB. The free NF-κB then translocates into the nucleus in order to activate genes with NF-κB binding sites. Therefore, the effect of KR-31360 on the nuclear translocation of NF-κB was first investigated by immunofluorescence staining, which revealed that LPS stimulation induced the translocation of part, but not all, of the NF-κB p65 subunit from the cytoplasm into the nucleus. The LPS-induced NF-κB p65 nuclear translocation was suppressed by KR-31360 (Fig. 3A). The DNA-binding activity of NF-κB was examined by gel shift assays. NF-κB DNA-binding activity was increased by LPS in BV-2 microglia cells, and this increase was attenuated by KR-31360 at 2 μM (Fig. 3B). The binding specificity of NF-κB was confirmed by supershift assay or using the unlabeled probe containing the NF-κB binding sequence. The effect of KR-31360 on MAP kinases (ERK, JNK, and p38), which are upstream signaling molecules in inflammatory reactions and mediate transcriptional changes in gene expression in response to LPS [30,31], was next examined. Western blot analysis was carried out using the antibodies against phospho-forms of the three MAPKs. The phosphorylation of each MAPK peaked at different time points. The phosphorylation levels of ERK, JNK, and p38 showed a peak at 60 min, 30 min, and 60 min after the addition of LPS, respectively (Fig. 3C, left). KR-31360 (2 μM) repressed the phosphorylation of JNK and ERK at the peak time point, whereas the phosphorylation of p38 was not significantly affected (Fig. 3C, right). The results indicate that KR-31360 inhibits NF-κB, JNK, and ERK pathways.

3.4. Cytoprotective effect of KR-31360 against microglia-mediated neuron cell death

As some of the inflammatory products of activated microglia contribute to neuronal death [32], the inhibition of microglial activation may protect neurons against the cytotoxic effect of activated microglia in the microglia/neuron coculture. Therefore, the potential protective effect of KR-31360 on microglial neurotoxicity was examined using a coculture of microglia and neuroblastoma cells. HAPI microglial cells (1.5×10^4 cells/well) were pretreated for 30 min with KR-31360 prior to the application of LPS. Then, the culture media were discarded and EGFP-expressing B35 (B35-EGFP) neuroblastoma cells (3.75×10^4 cells/well) and LPS were added. After additional incubation, B35-EGFP neuroblastoma cells were counted to assess cell viability. The coculture experiments revealed that LPS-activated microglia reduced the viability of B35-EGFP cells by ~50% compared to control culture of unstimulated microglia and B35-EGFP cells. KR-31360 attenuated the LPS/microglia-induced cell death of B35-EGFP neuroblastoma cells (Fig. 4). The viability of B35-EGFP was not affected by 100 ng/ml LPS alone without microglia coculture (data not shown). These results indicate that KR-31360 may be neuroprotective by suppressing microglial activation and subsequent neurotoxicity. In the next set of experiments, the potential therapeutic possibility of KR-31360 against activated microglia-mediated neuronal cell death was explored by treatment of the compound at different time points in regards to microglial activation. KR-31360 inhibited activated microglia-mediated neuroblastoma cell death 32.8 ± 13.2%, 5.5 ± 7.1%, and 1.9 ± 3.5% upon pretreatment before LPS challenge, cotreatment with LPS, and posttreatment after LPS challenge, respectively, as determined by MTT assay. Since the viability of microglia cells was not affected by LPS or KR-31360 (Fig. 1), the results of MTT assay reflect the viability of cocultured B35-EGFP neuroblastoma cells. For the coculture of primary microglia and primary cortical neurons, microglia (4×10^4 cells/well) were pretreated with KR-31360 for 30 min and washed to remove KR-31360. CMFDA-labeled primary cortical neurons (4×10^4 cells/well) and LPS were then added to microglia culture. After the chronic stimulation of microglia with LPS for 72 h, CMFDA-positive neuronal cells were counted. The viability of CMFDA-labeled neurons was reduced by ~50% compared to the control coculture of unstimulated microglia and neurons. KR-31360 attenuated neuronal cell death induced by the chronically activated microglia

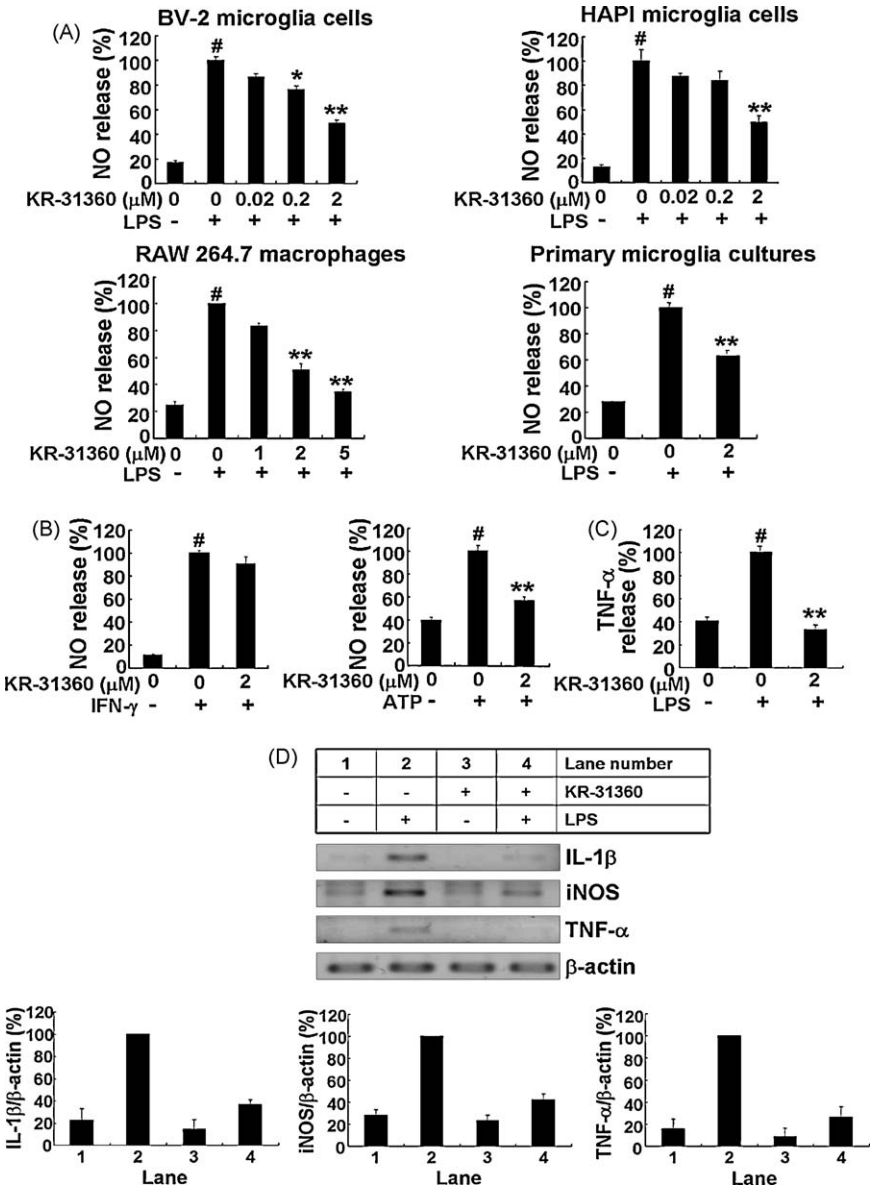

Fig. 2. KR-31360 inhibited NO production in BV-2 microglia cells, HAPI microglia cells, RAW 264.7 macrophage cells, or primary microglia cultures and expression of IL-1β, iNOS, and TNF-α in LPS-stimulated BV-2 microglia cells. Cells were left untreated or incubated with indicated concentrations or 2 μM of KR-31360 for 24 h in the absence or presence of 100 ng/ml LPS (A, C), 50 units/ml of IFN-γ or 2 mM of ATP (B). Cell culture media were collected and subjected to NO assay (A, B) or TNF-α sandwich ELISA (C), respectively. NO release was expressed as a percentage of NO production from LPS-, IFN-γ, or ATP-stimulated cells. The data were expressed as the mean ± S.D. ($n = 3$). $^{\#}P < 0.01$ vs. untreated control; $^{*}P < 0.05$, $^{**}P < 0.01$ vs. LPS, IFN-γ, or ATP alone. For RT-PCR analysis, cells were left untreated or incubated with 2 μM of KR-31360 for 6 h in the absence or presence of 100 ng/ml LPS. After treatment, total RNA was isolated and specific mRNA levels were determined by RT-PCR analysis (D; upper) and then subjected to densitometric quantification (lower). Levels of IL-1β, iNOS, and TNF-α were normalized to β-actin levels and expressed as a relative change in comparison to the LPS treatment, which was set to 100% (lane 2). Data from triplicate determinations are shown (mean ± S.D.).

(Fig. 4C). Moreover, the microglia-conditioned media, which were collected from LPS-treated primary microglia culture, also reduced the viability of primary neuron culture by ~30%. The reduced neuronal viability was recovered by treatment of microglia with KR-31360 under the similar condition (Fig. 4C). These results indicate that KR-31360 may be neuroprotective by suppressing microglial activation and subsequent neurotoxicity. However, the variability in the protective effects of the compound among different cell lines and primary cultures cannot be explained at present.

3.5. Inhibition of microglial activation by KR-31360 in a mouse neuroinflammation model

The effect of KR-31360 on microglial activation *in vivo* was determined by using a mouse neuroinflammation model. Histochemical detection of isolectin B4 (IB4) in brain tissues indicated that KR-31360 significantly inhibited LPS-induced microglial activation *in vivo* as evidenced by the decrease in the number of IB4-positive cells (Fig. 5). IB4 has been used as a specific marker for microglia. The number of IB4-positive cells was increased in mice injected with vehicle + LPS compared with control animals. The LPS-induced increase of IB4-positive cells was reduced in mice injected with KR-31360 + LPS. Fig. 5A shows representative image of IB4 staining of brain tissue sections. KR-31360 decreased the number of IB4-positive cells by 43% (Fig. 5B). Inhibition of microglial activation by KR-31360 was further supported by quantitative measurement of the expression of proinflammatory genes such as TNF-α, IL-1β, MCP-1, MIP-1α, and iNOS. RT-PCR analysis of brain tissues indicated that mRNA levels of these genes were increased by LPS, which was inhibited by KR-

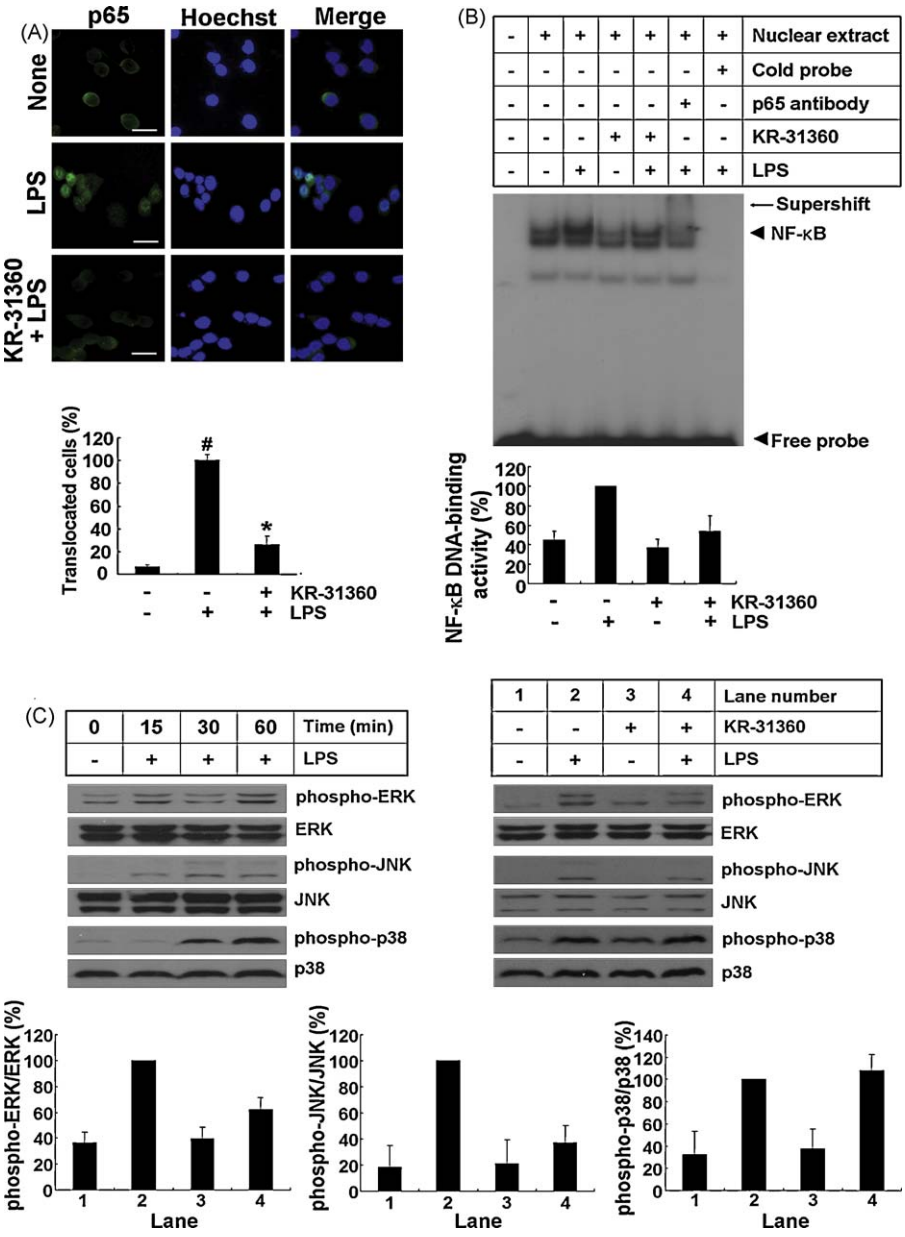

Fig. 3. KR-31360 suppressed NF-κB, ERK, and JNK activation in LPS-stimulated BV-2 microglia cells. Cells were stimulated with 100 ng/ml LPS in the absence or presence of KR-31360 (2 μM) that had been added 30 min before the stimulation. After 1 h, subcellular localization of NF-κB p65 subunit was examined by using immunofluorescence staining. LPS-induced NF-κB p65 nuclear translocation, which was colocalized with Hoechst staining, was inhibited by KR-31360. Representative images of the cells are shown (A; upper). Scale bar, 25 μm. The number of cells with p65 nuclear translocation was determined and the percentage of cells with p65 translocation was calculated (lower) (A). After LPS stimulation for 1 h, nuclear extracts were isolated for gel shift assay. LPS-induced NF-κB DNA binding activity (arrow head) was also inhibited by KR-31360 (B). Supershift was indicated by the arrow. The numbers indicate fold change of NF-κB complex as determined by densitometric analysis. The data were expressed as the mean ± S.D. ($n = 3$) (A). $^{\#}P < 0.01$ vs. untreated control; $^{*}P < 0.01$ vs. LPS only. For Western analysis, cells were pretreated with KR-31360 (2 μM) for 30 min and then stimulated with LPS (100 ng/ml) for 15, 30, or 60 min. Western blot analysis was then performed to evaluate the activation of MAP kinases. The phosphorylation of each MAPK peaked at different time points (C; left). The ERK and JNK phosphorylation was inhibited by KR-31360 at the peak time point. On the contrary, p38 phosphorylation was not significantly affected by KR-31360 (C; right). Quantification of phospho-MAP kinases was performed by normalization to each total-MAP kinase and expressed as a relative change in comparison to the LPS treatment, which was set to 100% (lane 2). Data from triplicate determinations are shown (mean ± S.D.).

31360 (Fig. 5C). Immunohistochemical detection of NeuN (marker for neuron-specific nuclear protein) indicated that LPS injection induced microglial activation, but not neuronal cell death, under the current experimental conditions (data not shown). LPS-induced febrile response may lead to microglial activation. However, the effect of KR-31360 on body temperature of the animals was not determined in the present study. It cannot be ruled out that the protective properties of the compound *in vivo* could be partly due to a potential hypothermic response it might induce.

3.6. Effect of KR-31360 on LPS-induced transcription profile in microglial cells

In order to further assess the effect of the compound on microglial signal transduction pathways associated with inflammatory activation, DNA microarray analysis was performed to obtain gene expression profile of microglia cells treated with LPS in the absence or presence of KR-31360. The dye-swap approach was used to remove dye bias. Based on the microarray analyses, 332 genes were consistently up-regulated more than 2 times by

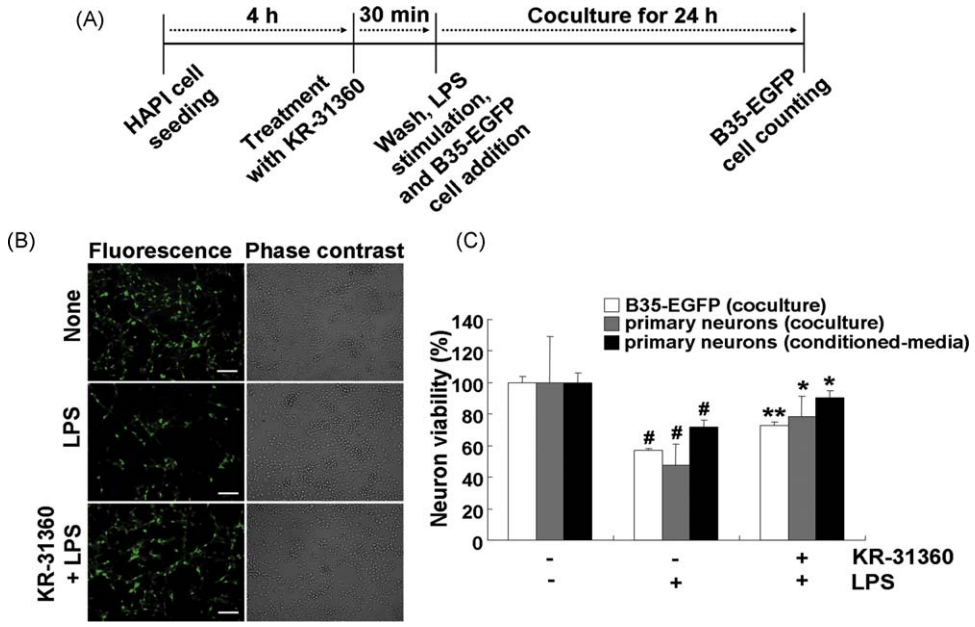

Fig. 4. KR-31360 attenuated microglial neurotoxicity. The effect of KR-31360 on the microglial neurotoxicity was examined using either the coculture of HAPI rat microglia and B35 neuroblastoma cells expressing EGFP (A–C), the coculture of primary microglia and primary neurons (C), or the addition of microglia-conditioned media to neuronal cultures (C). HAPI rat microglia cells were pretreated with 2 μM of KR-31360 for 30 min and washed with PBS. Then, LPS (100 ng/ml) and B35-EGFP rat neuroblastoma cells were added to microglia cells for coculture for 24 h (A). At the end of coculture, the number of viable B35-EGFP neuroblastoma cells in the five randomly chosen microscopic fields per well was counted under a fluorescence microscope (C; white bars). Representative fluorescence or phase contrast images of cells are shown (B). Scale bar, 100 μm. KR-31360 (2 μM) alone did not exert cytotoxicity against B35-EGFP neuroblastoma cells or any other cell types used in this study (Supplementary Fig. 4). For the coculture of primary microglia and primary neurons, microglia were pretreated with 2 μM of KR-31360 for 30 min. Then, LPS (100 ng/ml) and CMFDA-labeled primary neurons were added to microglia cultures. For the chronic activation of microglia, the culture media were replaced with fresh media containing LPS every 24 h, over 72 h. After LPS stimulation for 72 h, CMFDA-positive neurons were counted under a fluorescence microscope (C; gray bars). Microglia cultures were treated with LPS (100 ng/ml) in the absence or presence of 2 μM KR-31360 for 6 h. Culture media were removed, and fresh culture media were then added to microglia culture. After additional 24 h incubation, conditioned media were collected and added to primary neurons. After 24 h incubation, the viability of neurons was assessed by MTT assay (C; black bars). Results were expressed as a percentage of control (unstimulated microglia cultures + neuroblastoma or neurons) (mean ± S.D.). $^{\#}P < 0.01$ vs. control; $^{*}P < 0.05$, $^{**}P < 0.01$ vs. LPS only.

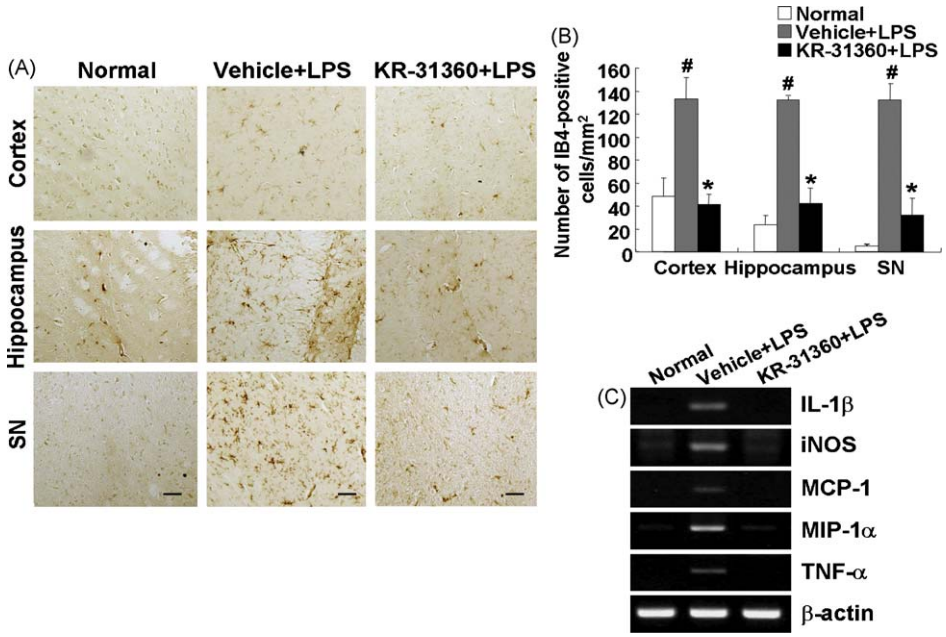

Fig. 5. KR-31360 inhibited microglial activation in a mouse neuroinflammation model. C57BL/6 mice were injected intraperitoneally with vehicle (PBS containing 0.5% DMSO) or KR-31360 (diluted in PBS) once daily at 20 mg/kg for 4 days. At 24 h after the first injection of vehicle or KR-31360, mice were intraperitoneally injected with 5 mg/kg LPS. Mice were anesthetized with diethyl ether and transcardially perfused with ice-cold saline 72 h after the LPS injection. Brains were removed and sections were stained with IB4 (a marker for microglia). IB4-positive cells were observed in cortex, hippocampus, and substantia nigra (SN) region of vehicle + LPS- or KR-31360 + LPS-injected mouse brains (A). Scale bar, 50 μm. The number of IB4-positive cell per mm^2 within the defined positions (see Section 2) was decreased by KR-31360 (B). The expression levels of proinflammatory genes were also reduced by KR-31360 as determined at 6 h after the LPS injection (C). The data were expressed as the mean ± S.D. (n = 3 per experimental group). $^{\#}P < 0.01$ vs. normal animals; $^{*}P < 0.01$ vs. vehicle + LPS-injected animals.

treatment with KR-31360, and 299 genes were down-regulated at least 1.5 times by the compound (Supplementary Fig. 1). The gene ontology (GO) terms of up- or down-regulated genes are shown in Supplementary Fig. 2. Two genes related to LPS/TLR4 pathway (IKKε and PPARα) and randomly selected two other genes (CDK4 and CK1ε) from the list of differentially expressed genes were subjected to RT-PCR validation in BV-2 cells (Fig. 6, left) or primary microglia cultures (Fig. 6, right). The results showed a consistent change in the gene expression levels between BV-2 cells and primary microglia cultures. It was also confirmed by RT-PCR analysis that IKKε was down-regulated and PPARα was up-regulated by KR-31360. Results of RT-PCR analysis for CDK4 and CK1ε were consistent with microarray analysis. It has been reported that IKKε mediates the catalytic activity that leads to phosphorylation of interferon regulatory factor 3 (IRF-3) through myeloid differentiation factor 88 (MyD88)-independent pathway in TLR4 signaling [33,34]. PPARα is thought to play a role as a negative regulator of MyD88-dependent NF-κB pathway in TLR4 signaling and inhibits the production of inflammatory response markers such as iNOS and metalloproteinases [35]. From the pathway analysis using GenPlex™ v3.0 software and the KEGG database, TLR signaling has been identified as one of the KEGG pathways that are modulated by the compound (Table 3). TLR4 initiates LPS-induced signal transduction pathway and leads to the expression of various inflammatory cytokines and reactive oxygen species in LPS-stimulated cells (Supplementary Fig. 3). Although a few components of TLR4 signaling pathway such as MD2 and TAB were transcriptionally up-regulated by KR-31360, the expression of most TLR4 pathway molecules was down-regulated by KR-31360 (Table 4). In conjunction with the modulation of IKKε and PPARα gene expression, these results suggest that KR-31360 might negatively regulate both MyD88-dependent and -independent pathways of TLR4 signaling.

Table 3
KEGG biological pathways for differentially expressed genes in KR-31360-treated microglia cells.

KEGG pathway name	Gene counts
MAPK signaling	60
Cytokine–cytokine receptor interaction	56
Calcium signaling	41
JAK-STAT signaling	31
Toll-like receptor signaling	30
Cell cycle	28
Oxidative phosphorylation	26

Genes identified by GenePix Pro 5.1 analysis were tested for overrepresentation within the pathways for the KEGG under the Fisher Exact test assumption. The number of differentially expressed gene that is involved in each pathway is provided.

3.7. Effect of KR-31360 on protein expression profile in microglial cells

To examine the effect of KR-31360 on microglial proteome, two-dimensional gel electrophoresis (2-DE) analysis was conducted. After 2-DE separation of BV-2 microglia cell lysates that were treated with or without KR-31360, the 2-DE gel images were subjected to quantitative analysis using Melanie v6.0 software. 2-DE separation of each sample was repeated three times and a synthetic image was made using Melanie v6.0 software for quantitative analysis of spot intensity. The gels were normalized according to the total quantity in valid spots: the raw quantity of each spot in a gel is divided by the total quantity of all the spots in the gels that have been included in the master gel. From 2-DE image analysis, approximately 1191–1494 spots were detected in each gel, among which 219 spots showed more than 1.2 fold change in the intensity between control and KR-31360-treated microglia cells. Some of these spots were identified by LC–MS/MS (data not shown). Results of quantitative analysis for randomly selected two protein spots [translationally controlled tumor protein (TCTP), nucleosides diphosphate kinase B (NDP kinase B)] are shown in Table 5. A representative image of 2-DE gels with these spots magnified is shown in Fig. 7. These results provide additional potential targets which KR-31360 may act on concurrently with TLR4 pathway. Although proteins identified by 2-DE analysis were not further investigated in the current work, the results suggest that KR-31360 may exert propound effects on the microglial proteome as well as transcriptome. A large scale comparative analysis of microglial transcriptome and proteome following KR-31360 treatment will be the subject of future studies.

4. Discussion

Neuroinflammation is a process that results primarily from an abnormally high or chronic activation of microglia. This overactive state of microglia results in increased levels of inflammatory and oxidative stress molecules, which can lead to neuronal damage or death. Therefore, inhibition of the excessive microglial activation might be a therapeutic approach to prevent the progression of neurodegenerative diseases. In order to discover novel compounds that have inhibitory activities against microglial activation and ultimately attenuate neuroinflammatory disease progression, cell-based screen of imidazo [4,5-b] pyridine compounds was done using a microglial cell line. Because NO is one of the main proinflammatory mediators and plays an important role in neuroinflammatory diseases, effects of the synthetic compounds on the NO production in

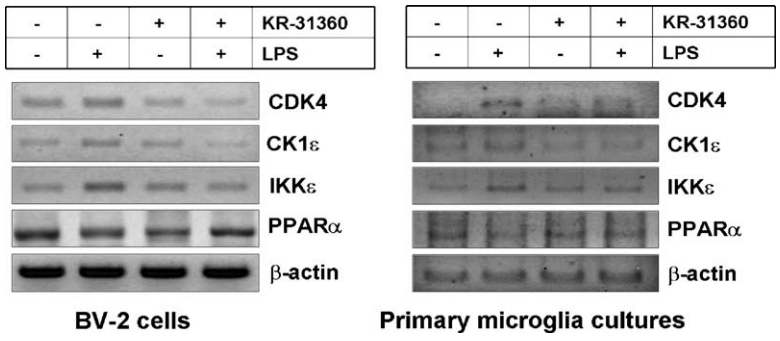

Fig. 6. Reevaluation of microarray-based differential gene expression by RT-PCR. BV-2 microglia cells (left) or primary microglia cultures (right) were left untreated or treated with KR-31360 (2 μM) for 4 h in the absence or presence of 100 ng/ml LPS. After treatment, total RNA was isolated and mRNA levels of specific genes were determined by RT-PCR. The expression of PPARα was up-regulated by KR-31360 in LPS-stimulated microglia. CDK4, CK1ε, and IKKε genes were down-regulated by KR-31360 in LPS-stimulated microglia.

Table 4
Genes differentially regulated by KR-31360 in TLR4 signaling pathway.

Functional family	Gene name	GenBank accession number	Description	(LPS + KR-31360)/ LPS ratio
Adaptors and TLR-interacting molecules	MD2	NM_016923	Lymphocyte antigen 96 precursor	1.54
	MyD88	AK090107	Myeloid differentiation primary response protein MyD88	0.71
Effector molecules	IRAK1	AY184362	Interleukin-1 receptor-associated kinase 1	0.84
	IRAK4	AK139992	Interleukin-1 receptor-associated kinase 4	0.80
	TAK1	AK133642	Mitogen-activated protein kinase kinase kinase 7	0.79
	TAB1	NM_025609	Mitogen-activated protein kinase kinase kinase 7 interacting protein 1	1.32
Downstream pathways molecules (NF-κB pathway)	IKKγ	AK037020	NF-kappa B essential modulator (NEMO)	0.69
	NF-κB	AK134081	Nuclear factor NF-kappa B p100 subunit	0.82
IRF pathway molecules	IKKε	AK220324	Inhibitor of nuclear factor kappa B kinase epsilon subunit	0.59
	IRF3	NM_016849	Interferon regulatory factor 3	0.77
JNK pathway molecules	MKK4/7	BC070467	Mitogen-activated protein kinase kinase 7	0.65
	JNK	AK145083	Mitogen-activated protein kinase 9	0.77

Table 5
Identification of differentially expressed proteins in KR-31360-treated BV-2 microglial cells.

Accession number	Protein name	Normalized density in control (mean ± S.D.)	Normalized density in KR-31360 (mean ± S.D.)	Ratio of KR-31360 vs control	Theoretical molecular weight (Da)	Theoretical p*I*
IPI00129685	TCTP	131.50 ± 31.82	60.01 ± 35.36	0.46	19462.17	4.76
IPI00127417	NDP kinase B	147.33 ± 38.21	95.00 ± 26.21	0.64	17345.30	6.97

Proteins separated by two-dimensional gel electrophoresis were identified by LC–MS/MS, following digestion with trypsin. After the peptide masses were matched with the theoretical peptide masses of all proteins from the International Protein Index mouse protein database (version 3.16) using the SEQUEST algorithm (Thermo Electron), selected proteins were identified. Abbreviations: IPI, international protein index; S.D., standard deviation; p*I*, isoelectric point.

LPS-stimulated BV-2 microglia cells were evaluated in the screen. Based on the strong inhibitory effect of KR-31360 on the NO production, further studies were focused on this compound. TNF-α and IL-1β are also major proinflammatory mediators and are implicated in the progression of neuroinflammatory diseases. The iNOS is capable of producing high amounts of NO that characterize inflammatory condition [36]. Therefore, effects of KR-31360 on these inflammatory mediators were investigated by ELISA or RT-PCR. These assays revealed that KR-31360 reduced the secretion of TNF-α and mRNA expression of TNF-α, IL-1β, and iNOS. Microglial activation also induces dynamic changes in cellular morphology, cell motility, and the organization of cytoskeletal proteins [37]. Therefore, the effect of KR-31360 on the actin cytoskeleton was also examined using rhodamine-conjugated phalloidin, which binds to actin filaments [38]. The intensity of phalloidin stain and size of cell bodies were reduced by the compound in activated microglia cells (Ock and Suk, unpublished results). These results suggest that KR-31360 may also inhibit actin polymerization, which in turn attenuates phagocytosis or migration of activated microglia.

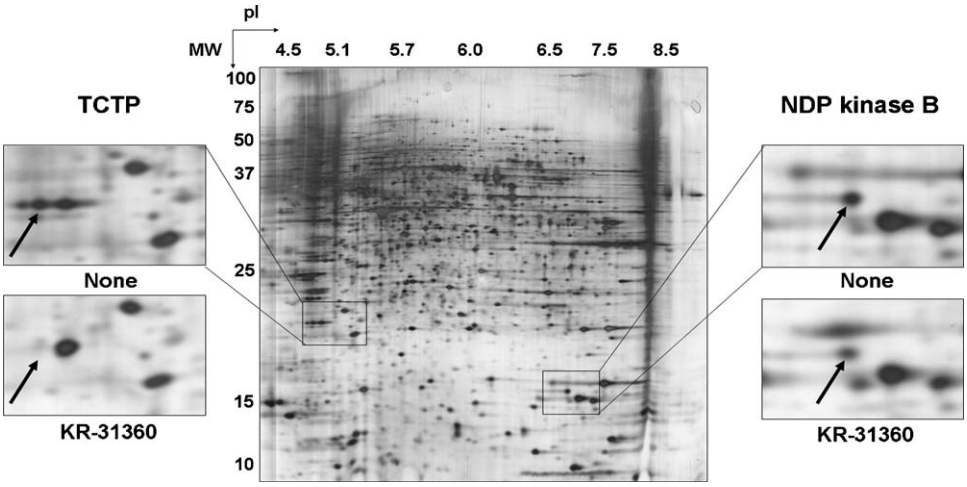

Fig. 7. A representative two-dimensional gel image of BV-2 microglia cells treated with KR-31360. The proteins were extracted from untreated or KR-31360 (2 μM)-treated BV-2 cells and separated by 2-DE. The electrophoresed gels were silver-stained. A representative gel image is shown. The identified proteins (TCTP and NDP kinase B) were marked by an arrow in the magnified image.

In the microglia–neuron coculture conditions, KR-31360 protected neurons against activated microglia-mediated neurotoxicity (Fig. 4). Since the KR-31360-pretreated microglia cultures were washed before the addition of the neuron cells for the coculture, B35 neuroblastoma cells and primary neurons were never exposed to KR-31360 in this coculture system. Therefore, the neuroprotective effect of KR-31360 is likely due to the inhibition of microglia activation, but not protective action on the neuron cells. The results of the coculture under different treatment conditions showed that pretreatment with KR-31360 was more effective in inhibiting microglial neurotoxicity than cotreatment or posttreatment, limiting the therapeutic potential of the compound. However, the compound can be used for the preventive purposes or may serve as a lead for further structural optimization in the drug development process. Although the coculture of LPS-stimulated microglia and neuroblastoma is not the same as *in vivo* conditions, it could mimic the pathological condition in neurodegenerative diseases where activated microglia contribute to neural damage. Moreover, the coculture system has been successfully used in the previous studies [15,39,40] to test the neuroprotective activity of the chemical compounds. Nevertheless, one could not exclude the possibility that the adhesion efficiency of neurons or neuroblastoma cells, which were added later than microglia, can be affected by the compound-treated microglia. To overcome the limitation of the *in vitro* coculture experiments, *in vivo* effect of KR-31360 on microglial activation was investigated in a mouse neuroinflammation model. In this study, KR-31360 exerted inhibitory effect on microglial activation by showing a decrease in the number of IB4-positive cells and inflammatory gene expression in brain tissues (Fig. 5). Although microglia are major immune cell types in the CNS, the possibility of contribution of other cell types to inflammatory gene expression cannot be excluded.

The results from gene-expression profile analysis and pathway analysis indicated that KR-31360 may inhibit microglial activation by suppressing upstream events of MAPKs and NF-κB pathways. In the microarray analysis, KR-31360 down-regulated the expression of IKKε and IRF-3. IKKε has been shown to be induced by LPS or inflammatory cytokines in RAW 264.7 macrophage cell line [41]. It has also been demonstrated that IKKε kinase activity and IRF-3 are required to produce interferon in response to LPS through a MyD88-independent pathway of TLR4 signaling [33,34]. In addition to IKKε and IRF-3, many components of TLR4 signaling pathway were down-regulated by KR-31360 in the microarray analysis (Table 4). On the other hand, PPARα was up-regulated in KR-31360-treated microglial cells. PPARα is a transcription factor belonging to the superfamily of ligand-activated nuclear receptors [42]. Previous studies have shown that PPARα interferes with the activation of inflammatory response genes such as iNOS and metalloproteinases by negatively regulating the NF-κB inflammatory transcription pathway in macrophages [35]. Moreover, PPARα showed neuroprotective effects by up-regulating brain antioxidant enzyme activity and by inhibiting inflammation pathways [43]. These findings suggest that the anti-neuroinflammatory effect of KR-31360 may also be mediated by the indirect effect of the compound on PPARα that suppresses NF-κB pathway.

Based on the proteomic analyses of microglia cells, TCTP and NDP kinase B were identified to be down-regulated by KR-31360. TCTP is highly conserved in all eukaryotic organisms and is ubiquitously expressed. TCTP levels are regulated in response to various extracellular stimuli. It has been reported that TCTP plays an important role in cell growth, cell cycle progression and malignant transformation [44]. In addition, TCTP has many cellular functions that are related with histamine-releasing factor activity and anti-apoptotic activity [45]. More recently, it has been reported that TCTP acts as a cytoplasmic repressor of Na^+,K^+-ATPase in HeLa cells and that overexpression of this protein *in vivo* leads to hypertension through the inhibition of vascular Na^+,K^+-ATPase activity and subsequent intracellular calcium mobilization and smooth muscle vasoconstriction [46]. However, physiological functions of TCTP are not fully understood at present. NDP kinase B (also known as nm23-M2) was initially known for its physiological function as an enzyme that participates in the synthesis of nucleoside triphosphates [47]. Previous studies showed that this protein has multiple functions such as cell differentiation, proliferation, and apoptosis [48,49]. NDP kinase B also played an important role as a protooncogene by positively regulating c-myc gene [50]. Its human homologue NM23-H2 was the most abundant transcripts overexpressed in colorectal carcinomas [51]. On the other hand, tumor suppressor activities of NM23-H2 have also been reported in various human cancers [52]. In a more recent study, NDP kinase B protected pro B cell line BAF3 from oxidative stress-induced cell death [53]. Although multiple functions of TCTP and NDP kinase B have been previously reported in various cell types, their role in microglia has never been investigated. In order to further understand the effects of KR-31360 on the intracellular signal transduction pathways of microglia, additional studies on these proteins and other microglial proteins showing differential expression profile are necessary. A limited literature search, however, suggests that cell growth or cell death/survival may be closely associated with the inhibitory effect of KR-31360 on microglial activation.

The imidazo [4,5-b] pyridine derivatives that were screened in this study were initially synthesized in order to develop angiotensin II receptor antagonists [10]. The imidazo [4,5-b] pyridine derivatives were synthesized by structural modifications at the imidazole 4- and 5-positions of Losartan (also known as DuP 753), which was developed as the first orally active nonpeptide angiotensin II receptor antagonists for various heart diseases such as hypertension and congestive heart failure [10]. Among these derivatives, two compounds (KR-31080 and KR-31103) maintained their binding affinity to angiotensin II receptor in binding assay and biological activity with potency similar to that of Losartan [10]. Other derivatives in the series had not been tested for their biological activity as angiotensin II receptor antagonists. The novel biological activity of KR-31360 as an inhibitor of microglial activation indicates a new therapeutic application of these compounds. The imidazo [4,5-b] pyridine derivatives screened in this study have an imidazopyridine ring as a common backbone structure. A number of synthetic chemical compounds were derived from this chemical structure and were investigated for the biological activities under various physiological or pathological conditions. For example, characteristics of imidazopyridine derivatives as potent inhibitors of iNOS have been previously reported [54]. Other chemical compounds that possess imidazopyridine ring also displayed the cardiotonic activity [55] as well as inhibitory activity against CDK activation [56] or proton pump [57]. Zolpidem, another imidazopyridine agent, has a sedative hypnotic property and has been used for the treatment of insomnia [58]. Based on the above mentioned reports, it is speculated that the imidazopyridine ring is important for the biological activities of these compounds. The present study indicates that the inhibition of microglial activation may be an additional biological activity of the compounds containing the imidazopyridine ring.

The major technical challenge during phenotype-based screening is the identification of the target protein(s) of the bioactive molecule. Affinity purification can be a powerful method for direct target identification. In an effort to identify the target protein(s) of KR-31360 by affinity purification, the structural modification of KR-31360 was carried out based on SAR studies of imidazo [4,5-b] pyridine derivatives. KR-31022, a hydroxyl

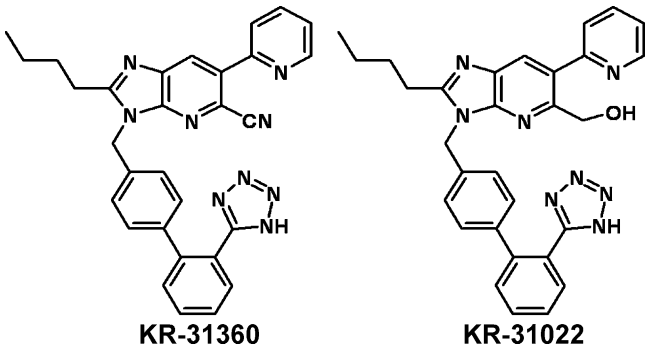

Fig. 8. The chemical structure of KR-31360 and KR-31022. The structure of KR-31360 (left) and its hydroxyl derivative KR-31022 (right) is compared.

Table 6
Comparison of IC_{50} values for KR-31360 and KR-31022 in microglial NO production.

Compound ID	IC_{50} for the inhibition of NO production (μM)
KR-31360	1.8 ± 0.3
KR-31022	>100

IC_{50} data for KR-31360 and KR-31022 were obtained from measurement of nitrite production in LPS-stimulated BV-2 microglia cells.

derivative of KR-31360, was synthesized by substitution of cyano group at the 6-position in KR-31360 with hydroxymethyl group, which a biotin moiety can be attached to (Fig. 8). In order to test whether the modified compound retains its biological activity, inhibitory effect of this derivative on LPS-stimulated NO production was investigated in BV-2 microglia cells. Unfortunately, the IC_{50} value of KR-31022 was greater than 100 μM (Table 6), thereby making it impossible to further proceed with this approach. Although the direct target protein of KR-31360 was not identified, the present study demonstrated that the inhibitory effect of KR-31360 toward microglial activation is mediated by negative regulation of TLR4 signaling pathway whose activation is related with inflammation responses. These activities of KR-31360 against TLR4 signaling pathways may be derived from transcriptional down-regulation of TLR4 signaling components: this possibility needs to be further explored in future studies. Nevertheless, the novel compound KR-31360 will be useful as a bioactive molecular probe and allows further analysis of the relationship between target processes/proteins and their cellular function. Also, the inhibitory effect of the KR-31360 against microglial activation suggests that this compound can be used for the development of novel preventive or therapeutic drugs against neuroinflammatory diseases.

Acknowledgements

This work was supported by the Korea Science and Engineering Foundation (KOSEF) grant funded by the Korea government (MEST) (No. 2009-0078941) and Bio R&D program through the Korea Science and Engineering Foundation funded by the Ministry of Education, Science and Technology (2008-04090).

Appendix A. Supplementary data

Supplementary data associated with this article can be found, in the online version, at doi:10.1016/j.bcp.2009.09.026.

References

[1] Block ML, Zecca L, Hong JS. Microglia-mediated neurotoxicity: uncovering the molecular mechanisms. Nat Rev Neurosci 2007;8:57–69.
[2] Liu B, Hong JS. Role of microglia in inflammation-mediated neurodegenerative diseases: mechanisms and strategies for therapeutic intervention. J Pharmacol Exp Ther 2003;304:1–7.
[3] Kreutzberg GW. Microglia: a sensor for pathological events in the CNS. Trends Neurosci 1996;19:312–8.
[4] Morgan SC, Taylor DL, Pocock JM. Microglia release activators of neuronal proliferation mediated by activation of mitogen-activated protein kinase, phosphatidylinositol-3-kinase/Akt and delta-Notch signalling cascades. J Neurochem 2004;90:89–101.
[5] Gonzalez-Scarano F, Baltuch G. Microglia as mediators of inflammatory and degenerative diseases. Annu Rev Neurosci 1999;22:219–40.
[6] Wyss-Coray T. Inflammation in Alzheimer disease: driving force, bystander or beneficial response? Nat Med 2006;12:1005–15.
[7] McGeer PL, McGeer EG. Inflammation and neurodegeneration in Parkinson's disease. Parkinsonism Relat Disord 2004;10(Suppl. 1):S3–7.
[8] Jack CS, Arbour N, Manusow J, Montgrain V, Blain M, McCrea E, et al. TLR signaling tailors innate immune responses in human microglia and astrocytes. J Immunol 2005;175:4320–30.
[9] O'Neill LA, Bowie AG. The family of five: TIR-domain-containing adaptors in Toll-like receptor signalling. Nat Rev Immunol 2007;7:353–64.
[10] Yoo SE, Kim SK, Lee SH, Yi KY, Lee DW. A comparative molecular field analysis and molecular modelling studies on pyridylimidazole type of angiotensin II antagonists. Bioorg Med Chem 1999;7:2971–6.
[11] Blasi E, Barluzzi R, Bocchini V, Mazzolla R, Bistoni F. Immortalization of murine microglial cells by a v-raf/v-myc carrying retrovirus. J Neuroimmunol 1990;27:229–37.
[12] Bocchini V, Mazzolla R, Barluzzi R, Blasi E, Sick P, Kettenmann H. An immortalized cell line expresses properties of activated microglial cells. J Neurosci Res 1992;31:616–21.
[13] Cheepsunthorn P, Radov L, Menzies S, Reid J, Connor JR. Characterization of a novel brain-derived microglial cell line isolated from neonatal rat brain. Glia 2001;35:53–62.
[14] Schubert D, Heinemann S, Carlisle W, Tarikas H, Kimes B, Patrick J, et al. Clonal cell lines from the rat central nervous system. Nature 1974;249:224–7.
[15] Zheng LT, Ock J, Kwon BM, Suk K. Suppressive effects of flavonoid fisetin on lipopolysaccharide-induced microglial activation and neurotoxicity. Int Immunopharmacol 2008;8:484–94.
[16] Saura J, Tusell JM, Serratosa J. High-yield isolation of murine microglia by mild trypsinization. Glia 2003;44:183–9.
[17] Araki W, Yuasa K, Takeda S, Shirotani K, Takahashi K, Tabira T. Overexpression of presenilin-2 enhances apoptotic death of cultured cortical neurons. Ann N Y Acad Sci 2000;920:241–4.
[18] Ock J, Lee H, Kim S, Lee WH, Choi DK, Park EJ, et al. Induction of microglial apoptosis by corticotropin-releasing hormone. J Neurochem 2006;98:962–72.
[19] Schreiber E, Matthias P, Muller MM, Schaffner W. Rapid detection of octamer binding proteins with 'mini-extracts', prepared from a small number of cells. Nucleic Acids Res 1989;17:6419.
[20] Qin L, Wu X, Block ML, Liu Y, Breese GR, Hong JS, et al. Systemic LPS causes chronic neuroinflammation and progressive neurodegeneration. Glia 2007;55:453–62.
[21] Cunningham C, Wilcockson DC, Campion S, Lunnon K, Perry VH. Central and systemic endotoxin challenges exacerbate the local inflammatory response and increase neuronal death during chronic neurodegeneration. J Neurosci 2005;25:9275–84.
[22] Shevchenko A, Wilm M, Vorm O, Mann M. Mass spectrometric sequencing of proteins silver-stained polyacrylamide gels. Anal Chem 1996;68:850–8.
[23] Kim S, Ock J, Kim AK, Lee HW, Cho JY, Kim DR, et al. Neurotoxicity of microglial cathepsin D revealed by secretome analysis. J Neurochem 2007;103:2640–50.
[24] Chang LC, Tsao LT, Chang CS, Chen CJ, Huang LJ, Kuo SC, et al. Inhibition of nitric oxide production by the carbazole compound LCY-2-CHO via blockade of activator protein-1 and CCAAT/enhancer-binding protein activation in microglia. Biochem Pharmacol 2008;76:507–19.
[25] Meng XL, Yang JY, Chen GL, Zhang LJ, Wang LH, Li J, et al. RV09, a novel resveratrol analogue, inhibits NO and TNF-alpha production by LPS-activated microglia. Int Immunopharmacol 2008;8:1074–82.
[26] Park JS, Woo MS, Kim DH, Hyun JW, Kim WK, Lee JC, et al. Anti-inflammatory mechanisms of isoflavone metabolites in lipopolysaccharide-stimulated microglial cells. J Pharmacol Exp Ther 2007;320:1237–45.
[27] Jin CY, Moon DO, Lee KJ, Kim MO, Lee JD, Choi YH, et al. Piceatannol attenuates lipopolysaccharide-induced NF-kappaB activation and NF-kappaB-related proinflammatory mediators in BV2 microglia. Pharmacol Res 2006;54:461–7.
[28] Jung HW, Chung YS, Kim YS, Park YK. Celastrol inhibits production of nitric oxide and proinflammatory cytokines through MAPK signal transduction and NF-kappaB in LPS-stimulated BV-2 microglial cells. Exp Mol Med 2007;39:715–21.
[29] Baeuerle PA, Henkel T. Function and activation of NF-kappa B in the immune system. Annu Rev Immunol 1994;12:141–79.
[30] Koistinaho M, Koistinaho J. Role of p38 and p44/42 mitogen-activated protein kinases in microglia. Glia 2002;40:175–83.
[31] Hommes DW, Peppelenbosch MP, van Deventer SJ. Mitogen activated protein (MAP) kinase signal transduction pathways and novel anti-inflammatory targets. Gut 2003;52:144–51.

[32] Stoll G, Jander S. The role of microglia and macrophages in the pathophysiology of the CNS. Prog Neurobiol 1999;58:233–47.
[33] Kawai T, Takeuchi O, Fujita T, Inoue J, Muhlradt PF, Sato S, et al. Lipopolysaccharide stimulates the MyD88-independent pathway and results in activation of IFN-regulatory factor 3 and the expression of a subset of lipopolysaccharide-inducible genes. J Immunol 2001;167:5887–94.
[34] Ikeda F, Hecker CM, Rozenknop A, Nordmeier RD, Rogov V, Hofmann K, et al. Involvement of the ubiquitin-like domain of TBK1/IKK-i kinases in regulation of IFN-inducible genes. EMBO J 2007;26:3451–62.
[35] Delerive P, De Bosscher K, Besnard S, Vanden Berghe W, Peters JM, Gonzalez FJ, et al. Peroxisome proliferator-activated receptor alpha negatively regulates the vascular inflammatory gene response by negative cross-talk with transcription factors NF-kappaB and AP-1. J Biol Chem 1999;274:32048–54.
[36] Beck KF, Eberhardt W, Frank S, Huwiler A, Messmer UK, Muhl H, et al. Inducible NO synthase: role in cellular signalling. J Exp Biol 1999;202:645–53.
[37] Bader MF, Taupenot L, Ulrich G, Aunis D, Ciesielski-Treska J. Bacterial endotoxin induces $[Ca^{2+}]_i$ transients and changes the organization of actin in microglia. Glia 1994;11:336–44.
[38] Huang ZJ, Haugland RP, You WM, Haugland RP. Phallotoxin and actin binding assay by fluorescence enhancement. Anal Biochem 1992;200:199–204.
[39] Kim S, Ock J, Kim AK, Lee HW, Cho JY, Kim DR, et al. Neurotoxicity of microglial cathepsin D revealed by secretome analysis. J Neurochem 2007.
[40] Zheng LT, Hwang J, Ock J, Lee MG, Lee WH, Suk K. The antipsychotic spiperone attenuates inflammatory response in cultured microglia via the reduction of proinflammatory cytokine expression and nitric oxide production. J Neurochem 2008;107:1225–35.
[41] Shimada T, Kawai T, Takeda K, Matsumoto M, Inoue J, Tatsumi Y, et al. IKK-i, a novel lipopolysaccharide-inducible kinase that is related to IkappaB kinases. Int Immunol 1999;11:1357–62.
[42] Teissier E, Nohara A, Chinetti G, Paumelle R, Cariou B, Fruchart JC, et al. Peroxisome proliferator-activated receptor alpha induces NADPH oxidase activity in macrophages, leading to the generation of LDL with PPAR-alpha activation properties. Circ Res 2004;95:1174–82.
[43] Deplanque D, Gele P, Petrault O, Six I, Furman C, Bouly M, et al. Peroxisome proliferator-activated receptor-alpha activation as a mechanism of preventive neuroprotection induced by chronic fenofibrate treatment. J Neurosci 2003;23:6264–71.
[44] Tuynder M, Susini L, Prieur S, Besse S, Fiucci G, Amson R, et al. Biological models and genes of tumor reversion: cellular reprogramming through tpt1/TCTP and SIAH-1. Proc Natl Acad Sci USA 2002;99:14976–81.
[45] Li F, Zhang D, Fujise K. Characterization of fortilin, a novel antiapoptotic protein. J Biol Chem 2001;276:47542–9.
[46] Kim MJ, Kwon JS, Suh SH, Suh JK, Jung J, Lee SN, et al. Transgenic overexpression of translationally controlled tumor protein induces systemic hypertension via repression of Na^+,K^+-ATPase. J Mol Cell Cardiol 2008;44:151–9.
[47] Parks RE, Agarwal RP. In: Boyer PD, editor. The enzymes, vol. 8. New York: Academic Press; 1973. p. 307–34.
[48] Amendola R, Martinez R, Negroni A, Venturelli D, Tanno B, Calabretta B, et al. DR-nm23 expression affects neuroblastoma cell differentiation, integrin expression, and adhesion characteristics. Med Pediatr Oncol 2001;36:93–6.
[49] Negroni A, Venturelli D, Tanno B, Amendola R, Ransac S, Cesi V, et al. Neuroblastoma specific effects of DR-nm23 and its mutant forms on differentiation and apoptosis. Cell Death Differ 2000;7:843–50.
[50] Postel EH, Berberich SJ, Flint SJ, Ferrone CA. Human c-myc transcription factor PuF identified as nm23-H2 nucleoside diphosphate kinase, a candidate suppressor of tumor metastasis. Science 1993;261:478–80.
[51] Zhang L, Zhou W, Velculescu VE, Kern SE, Hruban RH, Hamilton SR, et al. Gene expression profiles in normal and cancer cells. Science 1997;276:1268–72.
[52] Hartsough MT, Steeg PS. Nm23/nucleoside diphosphate kinase in human cancers. J Bioenerg Biomembr 2000;32:301–8.
[53] Arnaud-Dabernat S, Masse K, Smani M, Peuchant E, Landry M, Bourbon PM, et al. Nm23-M2/NDP kinase B induces endogenous c-myc and nm23-M1/NDP kinase A overexpression in BAF3 cells. Both NDP kinases protect the cells from oxidative stress-induced death. Exp Cell Res 2004;301:293–304.
[54] Tiso M, Strub A, Hesslinger C, Kenney CT, Boer R, Stuehr DJ. BYK191023 (2-[2-(4-methoxy-pyridin-2-yl)-ethyl]-3h-imidazo[4,5-b]pyridine) is an NADPH- and time-dependent irreversible inhibitor of inducible nitric-oxide synthase. Mol Pharmacol 2008;73:1244–53.
[55] Kelso EJ, McDermott BJ, Silke B. Differential effects of phosphodiesterase inhibitors on accumulation of cyclic AMP in isolated ventricular cardiomyocytes. Biochem Pharmacol 1995;49:441–52.
[56] Cai D, Byth KF, Shapiro GI. AZ703, an imidazo[1,2-a]pyridine inhibitor of cyclin-dependent kinases 1 and 2, induces E2F-1-dependent apoptosis enhanced by depletion of cyclin-dependent kinase 9. Cancer Res 2006;66:435–44.
[57] Berg AL, Bottcher G, Andersson K, Carlsson E, Lindstrom AK, Huby R, et al. Early stellate cell activation and veno-occlusive-disease (VOD)-like hepatotoxicity in dogs treated with AR-H047108, an imidazopyridine proton pump inhibitor. Toxicol Pathol 2008;36:727–37.
[58] Verster JC, Volkerts ER, Olivier B, Johnson W, Liddicoat L. Zolpidem and traffic safety—the importance of treatment compliance. Curr Drug Saf 2007;2:220–6.